

# Supplemental material for “New classical integrable systems from generalized $T\bar{T}$ -deformations”

Benjamin Doyon,<sup>1</sup> Friedrich Hübner,<sup>1</sup> and Takato Yoshimura<sup>2,3</sup>

<sup>1</sup>*Department of Mathematics, King’s College London, Strand, London WC2R 2LS, U.K.*

<sup>2</sup>*All Souls College, Oxford OX1 4AL, U.K.*

<sup>3</sup>*Rudolf Peierls Centre for Theoretical Physics, University of Oxford, 1 Keble Road, Oxford OX1 3NP, U.K.*

In this supplemental material, we refer to equations in the main text as  $(xMT)$  where  $x$  is the equation number.

## I. TWO-BODY SCATTERING IN THE SEMICLASSICAL BETHE SYSTEM

For two particles the evolution decouples in the trivial center of mass motion of  $x_1(t) + x_2(t)$  and the motion of the relative coordinate  $x_{12}(t) = x_1(t) - x_2(t)$ :

$$y_{12} + \theta_{12}t = x_{12}(t) + 2\partial_\theta\psi(x_{12}(t), \theta_{12}) := f(x_{12}(t)) \quad (1)$$

Note that  $f(x)$  is a one-dimensional function which satisfies  $f(x \rightarrow \pm\infty) \rightarrow \pm\infty$  since  $\psi_\theta(x, \theta)$  is bounded. Therefore for any time  $t$  a solution  $x_{12}(t)$  will always exist. If  $f(x)$  is monotone increasing, i.e.  $f'(x) = 1 + 2\psi_{x\theta}(x_{12}(t), \theta_{12}) > 0$  then this solution will also be unique for all times, otherwise not. This gives a bound  $\partial_x\partial_\theta\psi(x, \theta) > -\frac{1}{2}$ , which is automatically satisfied for positive  $\partial_x\partial_\theta\psi(x, \theta)(x, \theta)$ . Thus, given a positive phase shift  $\varphi(\theta)$  it is easy to find a  $\psi(x, \theta)$  that gives rise to unique trajectories, for instance  $\psi(x, \theta) = \frac{x}{2\sqrt{x^2 + \alpha^2}}\phi(\theta)$ , where  $\alpha > 0$  is an arbitrary real number and  $\phi'(\theta) = \varphi(\theta)$ . On the other hand, if  $\varphi(\theta)$  is negative, then non-uniqueness can easily happen if  $\partial_x\partial_\theta\psi(x, \theta)$  is too large. For instance, consider again the implementation  $\psi(x, \theta) = \frac{x}{2\sqrt{x^2 + \alpha^2}}\phi(\theta)$ : The trajectories are only unique if  $\alpha > |\varphi(\theta_{12})|$ , i.e. if the interaction region is broad. In fact, for fixed particle number  $N$  and bounded  $\varphi(\theta)$ , it is always possible to choose a  $\psi(x, \theta)$  with a sufficiently large interaction region, s.t. the trajectories are unique.

If  $\alpha$  is too small the inverse function of  $f$  becomes multivalued. In this case the trajectory becomes non-unique during scattering (see Fig. 1).

## II. SPECIALISATION TO HARD RODS

For hard rods of positive length  $\lambda$  [1], one may take the continuous piecewise linear  $\psi_{\text{hr},+}(x, \theta) = \{\frac{\lambda}{2} (x < -\lambda), -x/2 (|x| < \lambda), -\frac{\lambda}{2} (x > \lambda)\} \times \theta$ . The particles then trace the hard rods’ momenta. Indeed, this guarantees that whenever particles’ positions are separated by distances greater than  $\lambda$ , they move freely, while the first pair of particles coming to a distance  $\lambda$  experiences an instantaneous motion pass each other, effectively exchanging their positions. As almost surely (with respect

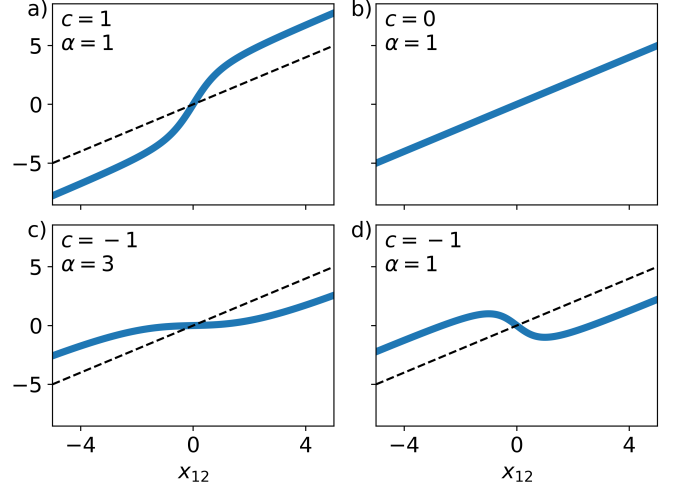


FIG. 1. Relation of the relative particle positions in free space  $y_{12} = y_1 - y_2$  and deformed space  $x_{12} = x_1 - x_2$  for different  $c$  and  $\alpha$  (in this case  $\partial_\theta\psi(x, \theta) = \frac{x}{\sqrt{x^2 + \alpha^2}}\varphi(\theta)$ , where  $\varphi(\theta) = \frac{2c}{\sqrt{c^2 + \theta^2}}$  is the Lieb-Liniger phase shift). The free particle solution b) for  $c = 0$  is given in the other plots for comparison (dashed line). For a) positive  $c > 0$  or c) large  $\alpha$  the map is invertible. If  $c < 0$  and  $\alpha$  too small then d) the map is non-invertible. This leads to the non-well definedness of particles during scattering.

to physically sensible distributions of positions and momenta) only at most one pair of particles at a time come to a distance  $\lambda$ , only at most one two-body process occurs at a time. This indeed reproduces the hard-rods dynamics. This should be seen as the limit  $\epsilon \rightarrow 0$  of the choice  $\psi_{\text{hr},+}^\epsilon(x, \theta) = \{\frac{\lambda}{2} (x < -(1 + \epsilon)\lambda), -\frac{x}{2(1 + \epsilon)} (|x| < \frac{\lambda}{2}), -\frac{\lambda}{2} (x > (1 + \epsilon)\lambda)\} \times \theta$ . This choice gives invertible Eqs. (2MT), (3MT) on all configurations where at most one pair of particles are a distance smaller than  $(1 + \epsilon)\lambda$ , and as  $\epsilon \rightarrow 0$ , at a collision of a pair of particles the speeds of the particles tend to infinity, giving, in the limit, the instantaneous exchange of their positions.

For hard rods of negative length  $-\lambda$  [2, 3] a natural choice would be  $\psi_{\text{hr},-}(x, \theta) = \frac{1}{2} \text{sgn}(x)\lambda\theta$ . In fact, the standard negative-length hard-rod model implements the negative lengths by allowing for rods’ centers to cross each other – thus being in the “wrong order” – up to a distance  $\lambda$  before changing direction; while here particles simply stick with each other for a time in order to implement the same overall scattering shift [4]. As the motion

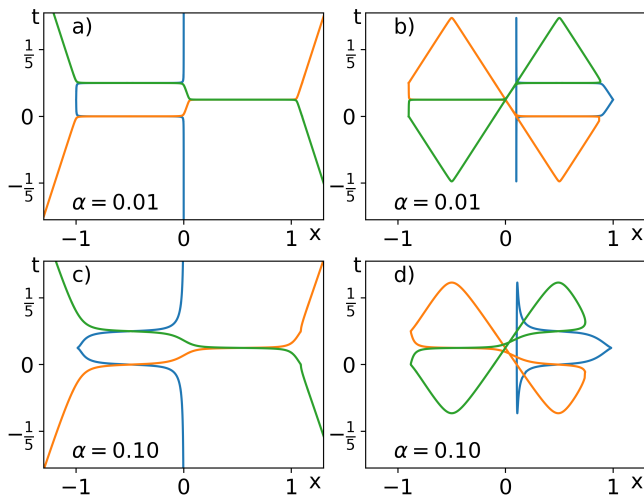


FIG. 2. Trajectories of three  $\lambda = 1$  hard rod like particles during scattering obtained by numerically solving (2MT). In order to have smooth behaviours, we regularize  $\psi_{\text{hr},+}(x, \theta)$  as follows  $\psi(x, \theta) = \frac{1}{4}(\sqrt{(x^2 - d^2)^2 + 4\alpha^2} - \sqrt{(x^2 + d^2)^2 + 4\alpha^2})$ , which reduces to  $\psi_{\text{hr},+}(x, \theta)$  as  $\alpha \rightarrow 0$ : a), b) depict the trajectories close to the hard rod limit while c), d) give smoother versions for comparison. The three particles are fixed at  $t = 0$  by  $y_1 = 0, \theta_1 = 0$  (blue),  $y_2 = 0, \theta_2 = 1$  (orange) and  $y_3 = 0.1, \theta_1 = -1$  (green). For both  $\alpha$  we find two solutions, the “normal sector” a), c) and the “vacuum loops” b), d).

of the particles stuck with each other simply takes the average momentum [4], in fact, this model represents the *center-of-mass position* of any group of rods in the wrong order; the microscopic dynamics is therefore slightly different.

In the case of positive-length rods, in fact there is one subtlety concerning the dynamics with  $\psi_{\text{hr},+}$ . Let us refer to the “normal sector” as the set of configurations under the constraint that all but at most one pair of particles are a distance strictly greater than  $\lambda$  from each other (or  $(1 + \epsilon)\lambda$  in the regularised version). Although the solutions to Eqs. (2MT), (3MT) in are indeed unique in the normal sector, *there are in general other solutions* where many particles are near to each other. These “ghost solutions” are not required for a well-defined dynamics when starting with configurations where all particles are far enough from each other, because, as explained above, almost surely the normal sector only is explored over time. However, if admitting all solutions, as per our general particle-production process, these solutions should be considered; they produce “vacuum” loops. Such loops in fact allow us to *define the hard-rod dynamics, for positive rod lengths  $\lambda$ , with rods being closer than a distance  $\lambda$ , thus in particular at densities higher than  $1/\lambda$ .*

Therefore, we see that the hard-rod model with positive rod lengths is that given by the restriction to the normal sector of the semiclassical Bethe systems with  $\psi_{\text{hr},+}$ ; this sector is almost surely invariant under the dynamics, hence a consistent restriction.

We note that the choice  $w(x, \theta) = \frac{1}{2}\delta(x)\theta$  in (5MT), for the generalised  $TT$ -deformation, corresponds to the mass-momentum deformation, argued in [2] to give rise to the hard rods. From our analysis, we see that a number of subtleties arise.

First, in [2], it is the analytical continuation in  $\lambda$ , from positive rod lengths, that was argued to give negative-length rods. Here, we see that, as per our discussion above, the direct deformation towards negative rod lengths gives  $\psi_{\text{hr},-}$ , the “center-of-mass” version where for groups of rods in the wrong order, we only trace the momentum of the center-of-mass position. Second, the choice  $w(x, \theta) = \frac{1}{2}\delta(x)\theta$ , in the direction of the  $TT$ -flow giving positive rod lengths, in fact only gives the true positive-length hard rods under the hard-core regularisation where exchanges are made at first collisions (see the main text); this was indeed the picture taken in [2]. Here, we see that one must choose a  $\lambda$ -dependent  $w_{\text{hr},+}(x, \theta) = \frac{1}{4\lambda}\Theta(|x| - \lambda)$  in order for  $TT$ -deformation to give the semiclassical Bethe system with  $\psi_{\text{hr},+}$  that directly represent, when restricting to the normal sector, the tracers of hard rods’ momenta (the go-through picture).

Finally, the specialisation of the finite-volume TBA equation (7MT) to the center-of-mass negative-length hard rods, with  $\psi_{\text{hr},-}$ , is

$$\varepsilon_L(x, \theta) = \beta\left(\frac{x}{L}, \theta\right) - \lambda \int \frac{d\theta'}{2\pi} e^{-\varepsilon_L(x, \theta')}. \quad (2)$$

It is interesting that we find no correction from the local structure at all: the same TBA equation arises at infinite volume. As (7MT) is derived in [5] under assumptions that are not satisfied for the positive-length hard rods,  $\psi_{\text{hr},+}$ , its specialisation to this case is not expected to give the correct answer (this turns out to be of a similar form to that of [6, 7], but slightly different).

### III. DETAILS ON THE NUMERICAL SIMULATIONS

In the letter we simulate the Euler scale time evolution of a macroscopic initial state described by:

$$\rho_0(x, \theta) = \frac{25}{2\pi} e^{-x^2/2} \left( e^{-25(\theta-1)^2/2} + e^{-25(\theta+1)^2/2} \right), \quad (3)$$

using both the underlying microscopic particle model and the GHD equation. In the following we provide details on both simulations.

#### A. Particle simulations

##### 1. Generating the initial state

In order to generate an initial state whose quasi-particle density corresponds to Eq. (3), we use an adaptation of an algorithm that is used to generate hard rods

initial states [8]. The algorithm first generates the positions of particles using their total density  $\bar{\rho}_0(x) = \int d\theta \rho_0(x, \theta) = \frac{10}{\sqrt{2\pi}} e^{-x^2/2}$  and then subsequently randomly chooses their initial  $\theta$  according to the double Gaussian momentum distribution  $f(\theta) = \frac{\rho_0(x, p)}{\bar{\rho}_0(x)} = \frac{1}{5\sqrt{2\pi}} \left( e^{-25(\theta-1)^2/2} + e^{-25(\theta+1)^2/2} \right)$ .

The procedure for generating the particle positions is as follows: Fix the location of the first particle (we choose  $x_1 = 0$ ). The locations of all the particles for  $x > 0$  are generated consecutively using the following rule:

$$x_{n+1} = x_n + \eta_n, \quad (4)$$

where  $\eta_n \sim \text{Exp}(L\bar{\rho}_0(x_n))$  are exponentially distributed random numbers. Note that this can be viewed as a discrete time random walk. As  $L \rightarrow \infty$  the  $\eta_n = \mathcal{O}(1/L)$  become very small, meaning one can ignore locally the  $x$  dependence of  $\bar{\rho}_0(x_n)$ . This stochastic process then locally generates a Poisson point process with the average density  $\bar{\rho}_0(x)$ . The slow dependence of  $\bar{\rho}_0(x)$  on  $x$  then creates variations of the density on the macroscopic scale. For practical purposes the procedure has to be stopped eventually, which we do once the density  $\bar{\rho}_0(x) < 0.01$  is below a threshold.

The above procedure generates the particle locations for  $x > 0$ . In order to generate the negative particle locations  $x < 0$  as well, we simply repeat the algorithm, but run it in the negative direction.

### B. Time evolution of the particles

The particles can then be time-evolved to any time  $t$  by solving Eq. (2MT) for given  $y_i(t) = y_i - \theta_i t$  numerically (the initial  $y_i$  can be computed from Eq. (2MT)). Numerically solving non-linear equations is a standard, but still non-trivial task. Appropriate methods could vary depending on the model, but here we choose to use the gradient descent algorithm. Its validity is guaranteed for models with positive phase-shifts, like the Lieb-Liniger phase shift – more precisely, whenever  $\partial_x \partial_\theta \psi(x, \theta) \geq 0$ . It is based on the observation that Eq. (2MT) is the minimization condition of the following convex function:

$$S(x_1, \dots, x_n) = \frac{1}{2} \sum_i (x_i - y_i)^2 + \frac{1}{2} \sum_{i \neq j} \gamma(x_i - x_j, \theta_i - \theta_j), \quad (5)$$

where  $\partial_x \gamma(x, \theta) = \partial_\theta \psi(x, \theta)$ . In our case  $\gamma(x, \theta) = \sqrt{x^2 + \alpha^2} \varphi(\theta)$ .

Since  $S(x_1, \dots, x_n)$  is a convex function the gradient descent algorithm for finding its minimizer is guaranteed to converge.

### C. GHD simulations

The GHD simulations were done using the IFluid package [9], which already implements the Lieb-Liniger model. The Euler scale GHD equation is solved using a Backward Semi-Lagrangian Implicit Runge-Kutta 4 method (this is a fourth order method, for details see [10]). The simulations were done on a space  $\times$  momentum =  $200 \times 200$  grid spanning  $x \in [-8, 8]$  and  $\theta \in [-2, 2]$ . Time is discretized in units  $\Delta t = 0.0025$ .

### IV. CHANGE OF METRIC AND PHYSICAL MOMENTUM DISTRIBUTION

Here we describe a different method to derive the GHD equation which is based on the change of coordinates Eq. (2MT). We can rewrite Eq. (2MT) directly in terms of the empirical density as (omitting the time argument)

$$\bar{y}_i = \bar{x}_i + \int d\bar{x} d\theta \rho_e(\theta, \bar{x}) \partial_\theta \psi(L(\bar{x}_i - \bar{x}), \theta_i - \theta) \quad (6)$$

where in particular we use the fact that  $\psi_\theta(0, 0) = 0$  by anti-symmetry. Assuming that  $\bar{x}_i = \bar{x}(\theta_i, \bar{y}_i)$  for some well-behaved function  $\bar{x}(\theta, \bar{y})$  and taking the large- $L$  limit,

$$\bar{y} = \bar{x}(\theta, \bar{y}) + \int d\bar{x}' d\theta' \rho_p(\theta', \bar{x}') \psi^{\text{sgn}(\bar{x}(\theta, \bar{y}) - \bar{x}')} \varphi(\theta - \theta'). \quad (7)$$

The differential at fixed  $\theta$  is

$$d\bar{y} = \left( 1 + \int d\theta' \rho_p(\theta', \bar{x}) \varphi(\theta - \theta') \right) d\bar{x} = 2\pi \rho_s(\theta, \bar{x}) d\bar{x} \quad (8)$$

where  $\rho_s(\theta, \bar{x})$  is the spatial, or total, density (with the conventional normalisation used in quantum systems). Eq. (8) is the transformation of coordinates  $\bar{x} \mapsto \bar{y}$  that is known to trivialise the GHD equation [11]. This trivialised GHD equation can be solved immediately and its solution can be mapped to the actual particle density by inverting Eq. (7). Thus, as the  $\bar{y}_i$  coordinates indeed evolve trivially, this can form a basis for an alternative way of proving the emergence of the GHD equation.

In fact, a similar calculation may be made to obtain the physical momentum density. Using

$$L \partial_x \psi(x, \theta) \Big|_{x=L\bar{x}} \rightarrow \delta(x) \phi(\theta) \quad (9)$$

where  $\phi(\theta) = \int_0^\theta d\theta' \varphi(\theta')$ , we get from (3MT)

$$\begin{aligned} p_i &= \theta_i + L \int d\bar{x} d\theta \rho_e(\theta, \bar{x}) \partial_x \psi(L(\bar{x}_i - \bar{x}), \theta_i - \theta) \\ &\rightarrow \theta_i + \int d\theta \rho_p(\theta, \bar{x}_i) \phi(\theta_i - \theta) \end{aligned} \quad (10)$$

from which we deduce  $p_i = p^{\text{Dr}}(\theta_i, \bar{x}_i)$  where  $p^{\text{Dr}}(\theta, \bar{x})$  is the Dressed momentum (see e.g. [12]); the latter is the

physical momentum variation upon adding a particle of rapidity  $\theta$  in Bethe ansatz systems (here in the state at macroscopic position  $\bar{x}$ ). Therefore, changing variable, the physical momentum distribution of our classical particle system is

$$\rho_{\text{phys}}(p, \bar{x}) = L^{-1} \sum_i \delta(\bar{x} - \bar{x}_i) \delta(p - p_i) = \frac{\rho_p(\theta(p, \bar{x}), \bar{x})}{2\pi \rho_s(\theta(p, \bar{x}), \bar{x})} \quad (11)$$

where we used  $2\pi \rho_s(\theta, \bar{x}) = \partial p^{\text{Dr}}(\theta, \bar{x}) / \partial \theta$ , and  $\theta(\cdot, \bar{x})$  is the inverse of  $p^{\text{Dr}}(\cdot, \bar{x})$ , i.e.  $p^{\text{Dr}}(\theta(p, \bar{x}), \bar{x}) = p$ . Using the expression for the occupation function  $n(\theta, \bar{x}) = \rho_p(\theta, \bar{x}) / \rho_s(\theta, \bar{x})$ , this reproduces the formula quoted in the main text.

## V. TRAJECTORIES FROM $T\bar{T}$ -DEFORMATIONS

In [5] we prove that the Hamiltonian Eq. (4MT) is well defined and arises from a generalised  $T\bar{T}$ -deformation of the system of free particles as per Eq. (6MT), under certain conditions on  $\psi$ , including  $\partial_x \partial_\theta \psi(x, \theta) \geq 0$ . There, we show that these conditions are sufficient to guarantee that Eqs. (2MT), (3MT) have unique solutions for  $\mathbf{x}$  and  $\boldsymbol{\theta}$ , respectively. If the conditions is broken, there is in fact no guarantee that Eq. (3MT) can be inverted to define the Hamiltonian as a function of  $\mathbf{x}, \mathbf{p}$ . Likewise, there is no guarantee that Eq. (2MT) can be inverted to provide the trajectories. Nevertheless, we discussed in the main text how to make sense of trajectories in cases where invertibility does not hold: Eq. (2MT) still defines the trajectories, but one must interpret it correctly; one interpretation is that one must modify phase space in order to account for different particle numbers, and particle creation / annihilation occurs.

Here, we show that, indeed,  $T\bar{T}$ -deformations of free-particle trajectories give Eq. (2MT) without further conditions on  $\psi(x, \theta)$ : *any solution to Eq. (2MT) is compatible with the corresponding generalised  $T\bar{T}$ -deformation, even when Eq. (2MT) is not invertible*. Thus, the interpretation above is sensible; in particular, one may augment the phase space, and at critical values of  $\lambda$ , where multiple solutions arise for some times, it is consistent to consider these multiple solutions at once, interpreted as the creation of particles and anti-particles. A similar construction from Eq. (3MT), to construct the full Hamiltonian on this larger phase space, is left for future works.

We note that the generalised  $T\bar{T}$ -deformation Eq. (5MT) can be obtained from the generator [2, 5, 13, 14]

$$X^\lambda(\mathbf{x}, \mathbf{p}) = - \sum_{ij} \int_{x_i}^{\infty} dz w(z - x_j, \theta_i^\lambda(\mathbf{x}, \mathbf{p}) - \theta_j^\lambda(\mathbf{x}, \mathbf{p})). \quad (12)$$

This is in the sense that the Hamiltonian is deformed as  $H_\lambda \rightarrow H_\lambda + \delta\lambda \{H_\lambda, X^\lambda\}$ . In fact, any conserved quantity transforms in this way, including the asymptotic momenta  $\theta_i^\lambda(\mathbf{x}, \mathbf{p})$ .

As the flow in  $\lambda$  is a Poisson flow, it preserves the Poisson algebra, thus it is natural to define the asymptotic impact parameters as those obtained from his flow:

$$y_i^\lambda(\mathbf{x}, \mathbf{p}) \rightarrow y_i^\lambda(\mathbf{x}, \mathbf{p}) + \delta\lambda \{y_i^\lambda(\mathbf{x}, \mathbf{p}), X^\lambda(\mathbf{x}, \mathbf{p})\}. \quad (13)$$

We now show that: *if Eq. (2MT) holds, in which we replace  $\psi \rightarrow \psi^\lambda = \lambda\psi$ , as well as  $y_i, \theta_i \rightarrow y_i^\lambda, \theta_i^\lambda$ , and if  $\theta_i^\lambda$ 's satisfy the flow equation (13), where the flow is defined using  $w = \partial_x \psi / 2$  (this is in agreement with Eq. (6MT))*. Therefore, any solution to Eq. (2MT) is compatible with the corresponding generalised  $T\bar{T}$ -deformation.

Note that we do not need to define the Hamiltonian for the above statement to make sense: we directly use the flow on trajectories, much as was done in [2]. Note also that under the above identification, we have the asymptotic condition  $|x|w(x, \theta) \rightarrow 0$  ( $|x| \rightarrow \infty$ ), thus the function  $X^\lambda(\mathbf{x}, \mathbf{p})$  is well defined. In fact it takes the form

$$X = \frac{1}{2} \sum_{ij} \psi(x_{ij}, \theta_{ij}) \quad (14)$$

where here and below we omit the superscript  $\lambda$  and use the condensed notation  $x_{ij} = x_i - x_j$ , etc., for lightness of notation.

The proof is as follows. Under the flow, the left-hand side of Eq. (2MT) gives (we use indices  $x, \theta$  to denote derivatives)

$$\{y_i, X\} = \sum_{jk} \{y_i, x_j\} \psi_x(x_{jk}, \theta_{jk}) + \sum_j \psi_\theta(x_{ij}, \theta_{ij}). \quad (15)$$

We may use Eq. (2MT) to obtain

$$\{y_i, x_j\} = \sum_l \psi_{\theta\theta}(x_{il}, \theta_{il}) \{\theta_{il}, x_j\} \quad (16)$$

whence

$$\{y_i, X\} = \sum_{jkl} \psi_{\theta\theta}(x_{il}, \theta_{il}) \psi_x(x_{jk}, \theta_{jk}) \{\theta_{il}, x_j\} + \sum_j \psi_\theta(x_{ij}, \theta_{ij}). \quad (17)$$

On the other hand, differentiating the right-hand side of Eq. (2MT), with  $\psi^\lambda = \lambda\psi$ , we obtain

$$\frac{\partial y_i}{\partial \lambda} = \sum_j \psi_\theta(x_{ij}, \theta_{ij}) + \sum_l \psi_{\theta\theta}(x_{il}, \theta_{il}) \frac{\partial \theta_{il}}{\partial \lambda}. \quad (18)$$

We evaluate the derivatives using the flow  $\partial \theta_i / \partial \lambda = \{\theta_i, X\}$ , to obtain

$$\frac{\partial \theta_{il}}{\partial \lambda} = \sum_{jk} \{\theta_{il}, x_j\} \psi_x(x_{jk}, \theta_{jk}). \quad (19)$$

Combining (17), (18) and (19), we find

$$\{y_i, X\} = \frac{\partial y_i}{\partial \lambda} \quad (20)$$

which shows the statement.

- 
- [1] H. Spohn, *Large Scale Dynamics of Interacting Particles* (Springer Berlin Heidelberg, 1991).
- [2] J. Cardy and B. Doyon, *JHEP* **2022**, 1 (2022).
- [3] P. A. Ferrari, C. Franceschini, D. G. Grevino, and H. Spohn, preprint arXiv:2211.11117 (2022).
- [4] B. Doyon and F. Hübner, preprint arXiv:2307.09307 (2023), arXiv:arXiv:2307.09307 [cond-mat.stat-mech].
- [5] B. Doyon, F. Hübner, and T. Yoshimura, “Generalised  $t\bar{T}$ -deformations of classical free particles,” (2023), arXiv:2312.14855 [cond-mat.stat-mech].
- [6] J. K. Percus, *J. Stat. Phys.* **15**, 505 (1976).
- [7] V. B. Bulchandani, preprint arXiv:2309.15846 (2023).
- [8] B. Doyon, G. Peretto, T. Sasamoto, and T. Yoshimura, *SciPost Phys.* **15**, 136 (2023).
- [9] F. S. Møller and J. Schmiedmayer, *SciPost Phys.* **8**, 041 (2020).
- [10] F. Møller, N. Besse, I. Mazets, H. Stimming, and N. Mauser, *Journal of Computational Physics* **493**, 112431 (2023).
- [11] B. Doyon, H. Spohn, and T. Yoshimura, *Nucl. Phys. B* **926**, 570 (2018).
- [12] P. Ruggiero, P. Calabrese, B. Doyon, and J. Dubail, *Phys. Rev. Lett.* **124**, 140603 (2020).
- [13] B. Pozsgay, Y. Jiang, and G. Takács, *JHEP* **2020**, 92 (2020).
- [14] J. Kruthoff and O. Parrikar, *SciPost Phys.* **9**, 78 (2020).